Matter and Radiation at Extremes | RESEARCH ARTICLE | scitation.org/journal/mre

Simulations of ALT-like explosive magnetic devices for ramp compression of materials by magnetically imploded liners

Cite as: Matter Radiat. Extremes 5, 047402 (2020); doi: 10.1063/1.5140621
Submitted: 5 December 2019 • Accepted: 17 May 2020 •
Published Online: 7 July 2020

A. M. Buyko,[a] G. G. Ivanova, and I. V. Morozova

AFFILIATIONS

FSUE, Russian Federal Nuclear Center – All-Russian Research Institute of Experimental Physics (RFNC-VNIIEF), Sarov, Nizhny Novgorod Region, Russia

Note: This paper is part of the Special Issue on the 11th International Conference on Dense Z-Pinches (DZP2019).
[a]**Author to whom correspondence should be addressed:** AMBuyko@vniief.ru

ABSTRACT

Revised simulations of ALT-like devices are presented. The results from these simulations closely match those from experiments and demonstrate the capabilities of the devices as applied to ramp compression of metals to pressures of 20 Mbar by imploding liners driven by ~10 MG azimuthal magnetic fields (with currents up to 55 MA). These results can be applied to the design of experiments on isentropic compression of materials.

I. INTRODUCTION

The Advanced Liner Technology (ALT)-3 device (Fig. 1) has been designed[1–4] to test the efficiency of the magnetic implosion of a cylindrical Al liner as an impactor driven up to 20 km/s by an azimuthal magnetic field $B_\varphi \sim 6$ MG (current ~70 MA). In the ALT-1,2 experiments[5] with a similar device and a 10-module disk explosive magnetic generator (DEMG), the same Al liner, having a thickness of 2 mm, was accelerated to 12 km/s (impact radius $R_{imp} = 1$ cm, field $B_\varphi \sim 2$ MG, current ~30 MA).

One-layer (Al, Cu) and two-layer liners are used.[1–9] The latter consist of an inner layer (impactor or tested material) and an adjacent highly conducting layer (Al, Cu pusher[6]), in which the current I(t) is flowing. The outer surface of the liner $R_{out}(t)$ is exposed to a magnetic field (1), which diffuses into the skin layer and produces the magnetic pressure (2):

$$B_\varphi(t) = I(t)/5R_{out}(t), \text{ [cm, MA, MG]} \quad (1)$$

$$P_B = B^2/8\pi, \text{ [MG, Mbar]}. \quad (2)$$

Devices such as the ALT-3 can be used to generate ramp pressures above 10 Mbar (Ref. 8) in materials by reducing the radii of the liner and the measuring units as a result of higher magnetic fields and, in particular, deeper implosion of the liners, such as the two-layer Al/Cu and Al/W liners with the parameters shown in (3). An increase in the relative thickness of such liners (with the mass being the same, ~20 g/cm) is expected to control the growth of their basic instabilities,[9] and with the height given above, the influence of the end walls (glide planes) on their implosion can be weakened.[10] Previous reports[7,8] have proposed studying ramp compression of such liners during their implosion using precision PDV measurements of the velocity $v_{in}(t)$ of the inner liner surface—this is analogous to the liner implosion experiments,[6] with the parameters shown in (4):

$$R_l = 30 \text{ mm}, \Delta_{Al} = 3.0 \text{ mm}, \Delta_{Cu(W)} = 0.34\,(0.16) \text{ mm},$$
$$H_l > 1.2\,R_i; R_{imp} = 1 \text{ mm}, R_{in0}/R_{imp} \sim 27, \quad (3)$$

$$R_l = 3.43\,(3.20) \text{ mm}, \Delta_{Al} = 1.0\,(1.2) \text{ mm},$$
$$\Delta_{Cu(Ta)} = 0.53 \mid (0.30) \text{ mm}; R_{imp} = 0.35 \text{ mm}, R_{in0}/R_{imp} \sim 5. \quad (4)$$

In this paper, we present revised simulations of the ALT-1–3 devices (Sec. II) and possible designs for the ALT-3 with different liner assemblies and measuring units (Sec. III). The 1D(MHD)$_n$ code that we used[11] was developed by Buyko, Ivanova, and Sofronov based on the UP-OK technique[13] and has been verified by a number of

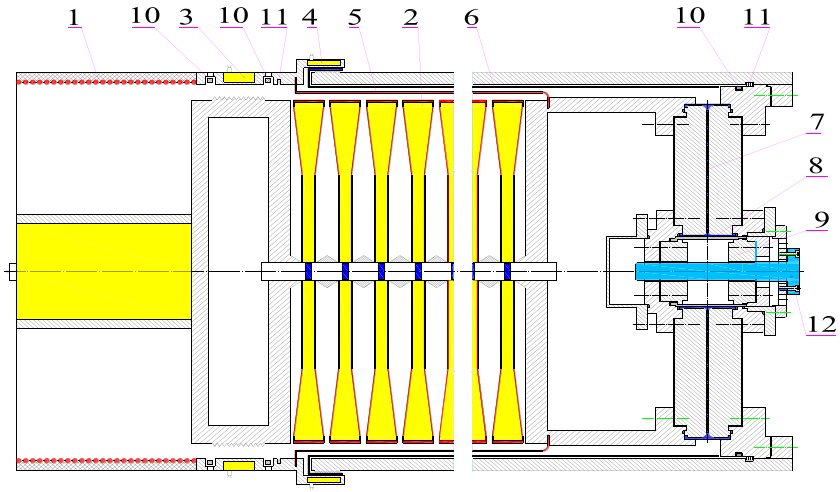

FIG. 1. Layout and basic parameters of the ALT-3 device (projected). 1 and 2: Ø0.4 m helical and 15-module disk explosive magnetic generators (HEMGs and DEMGs); 3 and 4: explosive closing switches (ECS)—crowbar 3 disconnects the HEMG at initial DEMG current I_0 = 7 MA ($t = t_0$); ECS 4, having low resistivity R_{kl}, connects a load of inductance L_0 = 6 nH at a given time t_{0l}, at fuse opening switch (FOS) voltage U_{0l} < 10 kV; 5: electrically exploded FOS with Cu foil of thickness Δ_f = 0.12–15 mm and height ~90 cm; 6 and 7: coaxial-radial transmission line (TL); 8: ponderomotive unit (PU) with an Al liner of outer and inner radius R_l = 4 cm and R_{in0} = 3.7 cm (Δ_{Al} = 3 mm) and height $H_l \sim 1.2R_i$; 9: PU end walls; 10 and 11: current probes; 12: measuring unit of radius R_{imp} = 1 cm (implosion depth R_{in0}/R_{imp} = 3.7) with photon doppler velocimetry (PDV) probes and test samples.

experiments.[5,12] Within the 1D-MHD simulation framework, we demonstrate the capabilities of the ALT-3-like devices as applied to isentropic compression of materials to pressures of 20 Mbar by magnetically driven liner implosion. To test these capabilities, one needs to perform similar[4,10] 2D-MHD simulations of the proposed liners taking into account the development of their basic instabilities and glide-plane effects. In such simulations, it is necessary to provide efficient implosion, which should be considerably deeper than that of the liners in (4) or the ALT-3 liner. Of even greater importance is experimental verification of the efficiency of the required deep liner implosion.

II. MODELING OF THE ALT-1–3 DEVICES

In the 1D(MHD)$_n$ code,[11] an arbitrary number (n) of 1D-MHD problems modeling major device components (Fig. 1) and coupled by boundary conditions of types (1) and (5) are solved in parallel. In the computational scheme of the devices under consideration, n = 13, and two interconnected current circuits are used: a DEMG-FOS with current $I_g(t)$ and an FOS-PU with current $I(t)$. Each circuit is composed of building blocks taken from "libraries" of energy sources (DEMG, FOS, etc.), transmission lines (coaxial, radial, etc.), and liner PUs (cylindrical, quasi-spherical, etc.). The currents $I_g(t)$ at $t > t_0$ and $I(t)$ at $t > t_{0l}$ are found from the equations of magnetic flux balance in the respective circuits (at $t < t_0$, the simulated HEMG current has a required maximum, I_0, which is important for providing the correct state of the Cu foil by the DEMG actuation time t_0). For the current $I(t)$, the circuit equation is given by (μs, nH, MA, kV)

$$d(LI)/dt = U_f - U_- = U_f - (U_{kl} + U_{tl} + U_{pu} + U_l),$$

$$t > t_{0l}, I(t_{0l}) = 0. \quad (5)$$

Here, $L(t)$ is the load inductance; $U_f(t)$ and $U_-(t)$ are the FOS foil voltage and the total rate of magnetic flux losses in the load: $U_{tl}(t)$ and $U_{pu}(t)$ on the TL and PU walls, $U_l(t)$ on the liner, and $U_{kl}(t) = R_{kl}(t)I(t)$ on the ECS [$R_{kl}(t)$ is taken from experiments]. To simulate the devices without ECS,[1,2] we assume that $t_{0l} = 0$ ($U_{0l} = 0$). These voltages and the change in the load inductance are calculated based on the outputs of respective 1D-MHD simulations: $U_i(t)$ is based on the electric fields $E_i(t)$ generated as a result of magnetic diffusion on the surface of the FOS Cu foil, on the TL and PU walls, and on the liner; $\Delta L(t)$ is based on the displacements of these walls $\delta_i(t)$ and the liner boundary $R_l - R_{out}(t)$. In the 1D-MHD simulations, the conductors are described by wide-range combinations of equation of state and conductivity—from their solid to their vaporized (Cu)[14] or plasma (Al, Cu)[15,16] state.

The revised simulations employ finer Lagrangian meshes with a mesh size of ~1 μm, which provide nearly converging simulation results. It is also important that they enable more consistent modeling of the load from the FOS to the liner (including magnetic flux losses and changes in its inductance). For example, eight 1D-MHD computations with the current $I(t)$ are used (previously six), including two to simulate the liner, the return conductor, and the insulators between them. The liner implosion simulations take into account radiation transfer in the "back and forth" approximation[17] along with electron heat conduction; the radiation flux across the outer liner surface is taken into account, but it has no effect on the insulator (an H-released discharge and current branch-off into it are possible, but, according to estimates, they have a minor effect on implosion). As in the previous simulations, five 1D-MHD problems simulate the DEMG-FOS system. Two problems with current $I_g(t)$ are used to model magnetic flux losses by diffusion into DEMG cavity walls and current conductors from there to the FOS; the essentially 2D motion of these walls is modeled by two functions, the minimum wall radius $R_{min}(t)$ (to calculate the losses mentioned above) and cavity inductance $L_g(t)$, which are taken from the DEMG "library" (they have been obtained in special 2D computations of cavity compression by the products of

explosion of the DEMG). Three problems are used to model the FOS as a multi-layer system that has three current-carrying inner layers with insulators between them (Fig. 1): the DEMG current conductor with current $I_g(t)$, the Cu foil with back current $I_g(t)$ and current $I(t)$, and the load current conductor with back current $I(t)$. The boundary conditions of these problems are interrelated and enable "through" 1D-MHD modeling of the whole system.

The ALT-1 and ALT-2 experiments demonstrated stable operation of the devices (with load currents reaching 31.5 ± 1.5 MA and 30.0 ± 1.3 MA)[5] and close agreement between the basic calculated characteristics and the results of previous simulations [Fig. 2(a)]. The results of the revised and previous simulations are nearly identical [Fig. 2(b)].

The revised and previous[4] simulations of the ALT-3 device differ notably [Figs. 3(a)–3(c)]. For example, the revised simulation gives the same DEMG current peak as before, 71 MA, but distinct differences in the FOS voltage and load current derivative, and a significant increase in the rate of magnetic flux losses in the load $U_{-}(t)$ along with an 11% decrease in its inductance at peak current. The peak current decreases weakly (62.7 MA at 7.5 nH instead of 64.1 MA at 8.4 nH), but the ramp pressure in the liner by the end of its implosion decreases by 14% (down to 0.97 Mbar), with nearly the same maximum liner velocity, ~21 km/s [Figs. 3(a), 3(b), and 3(d)]. Simulation 1 [Figs. 3(a)–3(d), dashed line], as our analysis shows, understated the inductance, and, in particular, the magnetic flux losses in the load, which resulted in overstated values of the peak current and magnetic pressure in the liner and its ramp pressure and velocity.

III. REVISED SIMULATIONS OF ALT-3-LIKE DEVICES

Results of such simulations of the devices with two-layer liners (3) are presented in Table I (simulations 1–4). They differ from the results of the same simulations reported from a previous study[8] more considerably than the similar computations of the ALT-3 device presented at the end of Sec. I. For example, at Cu foil thicknesses of 0.12–15 mm, the maximum current in the liners decreased by 12%–14% (previously 65–70 MA), which resulted in a decrease in the ramp pressures reached by the end of their implosion by 26%–29% in the W layer (previously 17.2–18.0 Mbar) and by 25%–27% in the Cu layer (previously 13.1–13.7 Mbar), respectively.

It is expected that this device will be able to use both Cu and Cu/W liners with the parameters in (6): "small copper PU" in the load with the previous load inductance (6 nH). The deepest implosion of such liners is achieved at an impact radius of R_{imp} = 0.7 mm, which seems to be feasible: it is twice the radius of the experimental measuring unit (4),

$$R_l = 20\ \text{mm}, \Delta_{Cu} = 2.0\ \text{mm}; \Delta_{Cu+W} = 1.75 + 0.25\ \text{mm};$$

$$R_{imp} = 1.0 - 0.7\ \text{mm}, R_{in0}/R_{imp} = 18 - 26. \quad (6)$$

The results of simulations 5–10 of such a device are presented in Table I and Figs. 4(a)–4(d). The DEMG currents and the FOS and load wall peak voltages in simulations 5–8 are close to those of simulations 1–4, and the liner currents have decreased by 5%–6%. The values of magnetic pressure in the copper skin layer, however, are nearly twice as high, which has increased attainable ramp pressures by a factor of 1.4–1.5.

At a Cu foil thickness of 0.15 mm [simulations 6(4w) and 8(4cu), Figs. 4(a)–4(d)], the values of attainable pressure and liner velocity are the highest, 19.7 Mbar and 14.5 Mbar, 29 km/s and 32 km/s, in the Cu/W and Cu liners at R_{in0}/R_{imp} = 26. The pressures reached at shallower implosion are lower, 16.1 Mbar and 12.3 Mbar at R_{in0}/R_{imp} = 18, but they are substantially higher than the pressures in the Al/W and Al/Cu liners (3) at their deeper implosion (12.8 Mbar and 9.9 Mbar, R_{in0}/R_{imp} ~ 27). Note that these pressures in the Cu/W liner are reached near the boundary of the W layer: in copper at R_{imp} = 1.0 mm and in tungsten at R_{imp} = 0.7 mm. Also note that the first electrical-explosion peak of FOS voltage is the highest in these simulations, at ~350 kV (the second peak is ~70 kV lower).

Decreasing the Cu foil thickness from 0.15 mm to 0.12 mm [simulations 5(2w) and 7(2cu) in Table I] enables preserving the attainable pressures at nearly the same level and significantly reducing the first peak of FOS voltage—by about 90 kV (so that it becomes 35–40 kV lower than the second peak of this voltage).

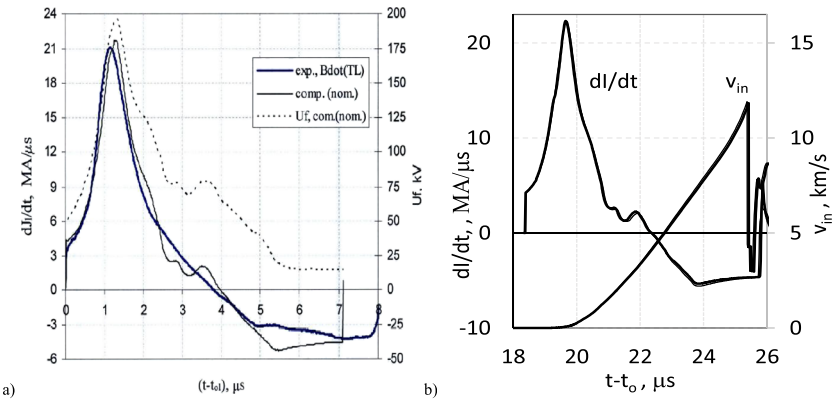

FIG. 2. (a) Load current derivative *dI/dt* in the ALT-2 experiment and in the previous simulation (heavy and fine lines, dashed line represents the calculated FOS voltage U_f); (b) *dI/dt* and inner liner surface velocity $v_{in}(t)$ in the revised and previous simulations (heavy and fine lines).

TABLE I. Results of simulations of devices with *Al/W* and *Al/Cu* liners (3), $R_{in0}/R_{imp} \sim 27$ (simulations 1–4) and simulations of devices with Cu/W and Cu liners (6), $R_{imp} = R_{in0}/R_{imp} =$ 18–26 (simulations 5–10). Here, Δ_f and U_{0l} are the Cu foil thickness and voltage at $t = t_{0l}$ (Fig. 1); I_g, $U_{f1} - U_{f2}$, and U_- are the maximum values of DEMG current and voltage on FOS (peaks 1 and 2) and load walls; I and L are the maximum current and respective load inductance; B and P_B are the highest magnetic field and magnetic pressure in the liner's skin layer; P_{ex}, P_{max}, and v_{max} are the pressures on the outer surface and inside the layer, and layer velocity at the end of implosion ($R_{in} = R_{imp}$).

Simulations	Δ_f mm	U_{0l} (kV)	I_g MA	$U_{f1} - U_{f2}$ kV	U_- (kV)	I (MA)	L (nH)	B (MG)	P_B (Mbar)	P_{ex} (Mbar)	P_{max} (Mbar)	v_{max} (km/s)
1(2W)	0.12	6	66	250–277	118	57	7.6	8.0	2.57	11.8	12.7	28
2(4W)	0.15	6	77	337–262	132	60	6.8	7.6	2.32	11.8	12.8	29
3(2Cu)	0.12	6	66	250–277	118	57	7.6	7.9	2.46	8.5	9.8	32
4(4Cu)	0.15	6	77	337–262	132	60	6.8	7.5	2.22	8.5	9.9	32
5(2w)	0.12	6	62	263–298	115	52	7.9	10.7	4.56	15.7–19.0	15.7–19.0	25–27
6(4w)	0.15	6	75	351–279	131	55	7.0	10.5	4.39	16.1–19.5	16.1–19.7	26–28
7(2cu)	0.12	6	62	265–304	114	51	8.0	10.8	4.64	⋯	11.6–13.5	28–30
8(4cu)	0.15	6	75	352–283	131	55	7.0	10.6	4.47	⋯	12.3–14.5	30–33
9($2w_0$)	0.12	0	63	385–375	117	49	9.2	11.0	4.81	11.8–13.6	11.9–14.1	21–23
10($4w_0$)	0.15	0	78	452–295	137	53	8.0	10.9	4.73	14.4–17.6	14.6–17.6	23–25

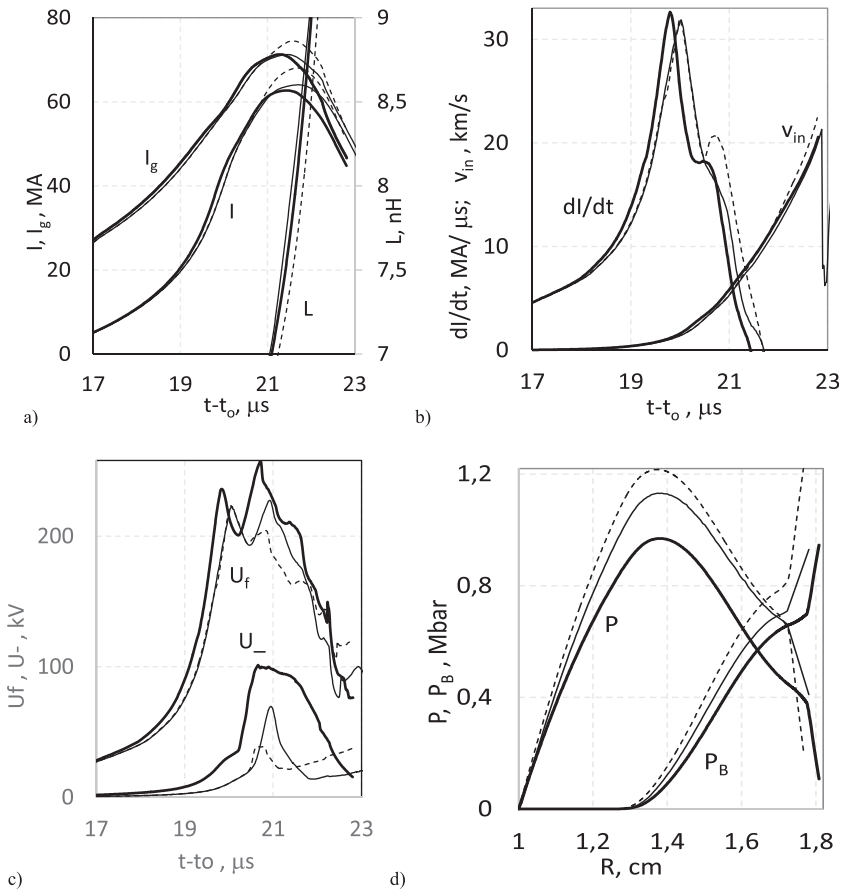

FIG. 3. Results of revised simulation of the ALT-3 device (heavy lines), previous simulation (fine lines), and simulation 1 (dashed line): (a) currents $I_g(t)$ and $I(t)$ and inductance $L(t)$ in the load; (b) current derivative dI/dt and velocity of the inner liner surface $v_{in}(t)$; (c) FOS voltage $U_f(t)$ and rate of magnetic flux losses in the load $U_-(t)$; (d) profiles of ramp $P(r)$ and magnetic $P_B(r)$ pressures in the liner at the end of implosion ($R_{in} = R_{imp} = 1$ cm).

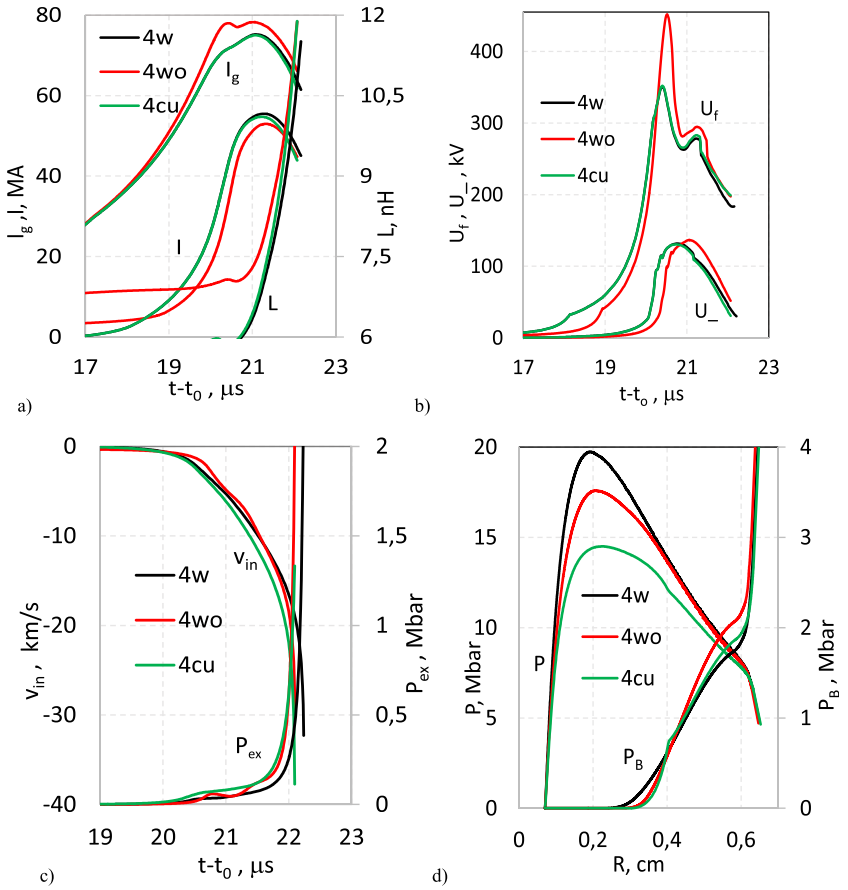

FIG. 4. Results of device simulations with Cu/W and Cu liners (6) at FOS Cu foil thickness of 0.15 mm [nos. 6(4w), 8(4cu), and 10(4w$_0$) in Table I]. (a) Currents in DEMG $I_g(t)$ and liner $I(t)$, load inductance $L(t)$; (b) voltages on foil $U_f(t)$ and load walls $U_-(t)$; (c) pressure $P_{ex}(t)$ on the outer boundary $R_{ex}(t)$ of the tested liner layer and velocity $v_{in}(t)$ of the inner boundary $R_{in}(t)$ of this layer; (d) profiles of ramp $P(r)$ and magnetic $P_B(r)$ pressures in the liner at the end of implosion ($R_{in} = R_{imp} = 0.7$ mm).

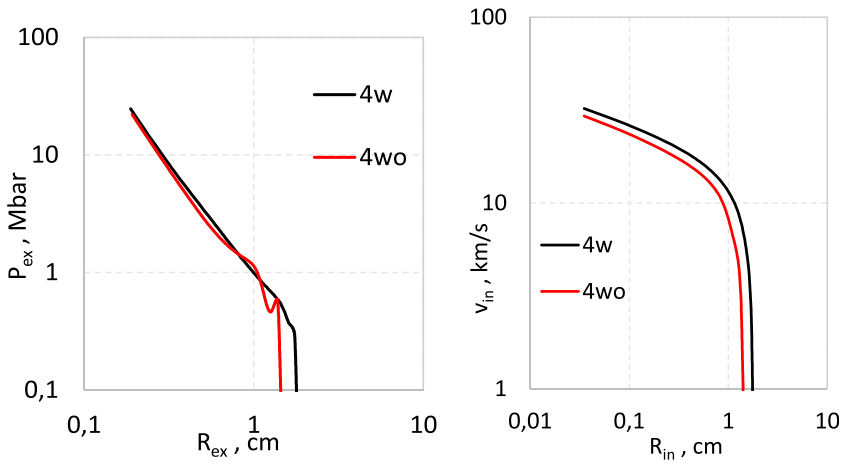

FIG. 5. (P_{ex} vs R_{ex}) and (v_{in} vs R_{in}) plots of the outer and inner boundaries of the liner's tested W layer from simulations 6(4w) and 10(4w$_0$), see Table I and Fig. 4.

Excluding the ECS—which would simplify the design significantly—would not result in any significant decrease in attainable pressures, but the first FOS voltage peaks would grow substantially, by 100–120 kV [simulations $9(2w_0)$ and $10(4w_0)$, Figs. 4(a), 4(b), and,4(d)].

Note that the pressures $P_{ex}(t)$ on the outer surface of the liner's tested W layer and the velocities $v_{in}(t)$ of the inner boundary of this layer—at early implosion times, at $P_{ex}(t) < 0.3$ Mbar—have a two-wave structure [Fig. 4(c)]. This is created by MHD processes in the liner's skin layer and is particularly visible in the ECS-free devices. These pressures P_{ex} and velocities v_{in} grow with the decreasing radius of the corresponding boundaries during implosion (Fig. 5), approximately as $P_{ex} \sim (R_{ex})^{-2.0}$ and $v_{in} \sim (R_{in})^{-0.2}$ at $R_{in} < 0.17$ mm (cumulation). This can decrease the accuracy of computational analysis of the liner velocities $v_{in}(t)$,[6,7] which is necessary for studying the isentropes of the tested materials, especially for the highest attainable pressures.

IV. CONCLUSION

Section I provides a summary of the numerical code used to simulate the devices of interest and to revise the simulations of their liner load. The revised and previous simulations of the experimental ALT-1,2 devices give practically the same results. The revised simulation of the ALT-3 device (design project) gives similar values of the load current, ~63 MA, and Al liner velocity, ~21 km/s ($R_l = 40$ mm, $\Delta_{Al} = 3$ mm, $R_{imp} = 10$ mm), as the previous simulation, but with a 14% decrease in ramp pressure to ~1 Mbar, which is achieved at an implosion depth of $R_{in0}/R_{imp} \sim 4$.

Section II reports the revised simulations of the ALT-3-like devices—first with the parameters of the two-layer Al/W and Al/Cu liners of $R_l = 30$ mm, $\Delta_{Al} = 3.0$ mm, $\Delta_{Cu(W)} = 0.34(0.16)$ mm, $R_{imp} = 1$ mm ($R_{in0}/R_{imp} \sim 27$). Their results differ substantially from the similar previous computations. For example, for a Cu foil thickness of 15 mm, the maximum liner current decreased by 14%, which resulted in a drop of ramp pressures reached in the W layer by 29% (to 12.8 Mbar). Next, we considered similar devices with Cu and Cu/W liners of $R_l = 20$ mm, $\Delta_{Cu} = 2.0$ mm, $\Delta_{Cu+W} = 1.75 + 0.25$ mm, $R_{imp} = 1.0$–0.7 mm, $R_{in0}/R_{imp} = 18$–26. Their current decreased to 55 MA (by 5 MA), but the magnetic pressures grew to 4.5 Mbar (nearly doubling), and the attainable ramp pressures increased by approximately half. The maximum ramp pressure of 19.7 Mbar was reached in the Cu/W liner at $\Delta_f = 0.15$ mm and an implosion depth of $R_{in0}/R_{imp} = 26$ ($v_{imp} = 29$ km/s). At $R_{in0}/R_{imp} = 18$, the pressure was lower, 16.1 Mbar, but this substantially exceeds the pressure in the *Al/W* liner at its deep implosion (see above). Reducing the thickness of the Cu foil from 0.15 mm to 0.12 mm, one can deliver nearly the same attainable pressures and bring the FOS peak voltage down to 90 kV. In the absence of the ECS, which would simplify the design significantly, there was no prominent decrease in the liner currents and pressures, but the FOS voltage peak grew substantially, from 350 kV to 450 kV.

The pressures $P_{ex}(t)$ on the outer surface of the liner's tested layer and the velocities $v_{in}(t)$ of this layer—at early implosion times, at $P_{ex}(t) < 0.3$ Mbar—have a two-wave structure, which becomes particularly clear in the ECS-free devices. These pressures P_{ex} and velocities v_{in} grow with the decreasing radius of the corresponding boundaries during implosion, approximately as $P_{ex} \sim (R_{ex})^{-2.0}$ and $v_{in} \sim (R_{in})^{-0.2}$ at $R_{in} < 0.17$ mm (cumulation). This can decrease the accuracy of computational analysis of the liner velocities $v_{in}(t)$, which is necessary for studying the isentropes of the tested materials, especially at the highest attainable pressures.

Our results can be applied to the design of experiments on isentropic compression of materials up to pressures ~20 Mbar.

ACKNOWLEDGMENTS

The authors thank S. F. Garanin, S. D. Kuznetsov, and V. B. Yakubov for useful discussions.

REFERENCES

[1]A. M. Buyko, Yu. N. Gorbachev, and G. G. Ivanova *et al.*, "Devices with disk explosive magnetic generators for high-velocity condensed-matter liner implosion," in *Proceedings of the XII International Conference on Megagauss Magnetic Fields Generation and Related Topics Novosibirsk, 2008*, edited by G. A. Shvetsov (SB RAS, Novosibirsk, 2010), pp. 475–485 (in Russian).

[2]A. M. Buyko, S. F. Garanin, Yu. N. Gorbachev *et al.*, "Explosive magnetic liner devices to produce shock pressures up to 3 TPa," in *Digest of Technical Papers of the 17th IEEE International Pulsed Power Conference*, edited by F. Peterkin and R. Curry (IEEE, S.I., Washington, DC, USA, 2009), pp. 215–220.

[3]A. M. Buyko, S. F. Garanin, A. M. Glybin *et al.*, "A disk EMG system for driving impacting liners to ~20 km/s," in *Digest of Technical Papers, 18th IEEE International Pulsed Power Conference* (IEEE, Chicago, USA, 2011), pp. 1330–1335.

[4]A. M. Buyko, S. F. Garanin, A. M. Glybin *et al.*, "Testing and revision of the parameters of a system for liner driving to 20 km/s," J. Appl. Mech. Tech. Phys. **56**(1), 96–102 (2015).

[5]A. M. Buyko, Yu. N. Gorbachev, V. V. Zmushko *et al.*, "Simulation of Atlas parameters in explosive magnetic experiments ALT-1,2," in *Proceeedings of 9th International Conference on Megagauss Magnetic Field Generation and Related Topics, M. –St. Petersburg, 2002*, edited by V. D. Selemir and L. N. Plyashkevich (VNIIEF, Sarov, 2004), pp. 747–751.

[6]R. W. Lemke, D. H. Dolan, D. G. Dalton *et al.*, "Probing off-Hugoniot states in Ta, Cu, and Al to 1000 GPa compression with magnetically driven liner implosions," J. Appl. Phys. **119**, 015904 (2016).

[7]S. D. Kuznetsov, A. M. Buyko, S. F. Garanin *et al.*, "Simulation of isentropic compression of aluminum by magnetically imploded liners in experiments ALT-1-3," No. MG-2018.

[8]A. M. Buyko, "Some promises of magnetic implosion of high-velocity condensed-matter liners in the ALT-3 driver," IEEE Trans. Plasma Sci. **46**(10), 3512–3517 (2018).

[9]A. M. Buyko, V. A. Vasyukov, S. F. Garanin *et al.*, "Possibility of the investigation of condensed liner magnetic implosion instability in the experiments with disk EMG," in *20th IET Symposium on Pulsed Power 2007* (STFC Rutherford Appleton Laboratory, Oxfordshire, UK, 2007), pp. 133–138.

[10]A. M. Buyko, "Simulations of the interaction of high-velocity condensed-matter liners with current-carrying walls," in *Proceedings International Conference 18th Khariton Scientific Talks on High Energy Density Problems* (FSUE RFNC-VNIIEF, Sarov, 2016), Vol. 1, pp. 307–317 (in Russian) [IEEE Trans. Plasma Sci. **45**(10), 2701–2706 (2017)].

[11]A. M. Buyko, "Disc explosive magnetic generator and quasi-spherical liner simulations with a 1D code," in *Proceedings 2006 International Conference on Megagauss Magnetic Field Generation Related Topics, November 5–10, 2006, Santa Fe, NM, USA*, edited by G. F. Kiuttu, P. J. Turchi, and R. E. Reinovsky (IEEE, Inc., 2007), pp. 287–292.

[12]A. M. Buyko, "Electrically exploded opening switches for high-current explosive magnetic generators," J. Appl. Mech. Tech. Phys. **56**(1), 114–124 (2015).

[13]N. F. Gavrilov, G. G. Ivanova, V. I. Selin, and V. N. Sofronov, "The UP-OK program for 1D continuum mechanics simulations within a 1D code," VANT,

Ser.: Codes Prog. Numer. Simul. Comput. Phys. Probl. **3**(4), 11–14 (1982) (in Russian).
[14]Yu. D. Bakulin, V. F. Kuropatenko, and A. V. Luchinsky, "Magnetohydrodynamic simulation of exploding wires," ZhTF **46**(9), 1963–1969 (1976) (in Russian).
[15]A. M. Buyko, S. F. Garanin, V. A. Demidov *et al.*, "Investigation of the dynamics of a cylindrical exploding liner accelerated by a magnetic field in the megagauss range," in *Megagauss Fields and Pulsed Power Systems*, edited by V. M. Titov and G. A. Shvetsov (Nova Science Publishers, New York, 1990), pp. 743–748.
[16]S. F. Garanin and V. I. Mamyshev, "Cooling of magnetized plasma at its interface with an exploding metal wall," PMTF **1**, 30–37 (1990) (in Russian).
[17]Ya. B. Zel'dovich and Yu. P. Raizer, *Physics of Shock Waves and High-Temperature Hydrodynamic Phenomena* (Nauka, Moscow, 1966) (in Russian).